Hybrid Algorithm and Active Filtering Dedicated to the Optimization and the Improvement of Photovoltaic System Connected to Grid Energy Quality

Imad Aboudrar*, Soumia El Hani*, Hamza Mediouni*, Najib Bennis*, Amina Echchaachouai*

*Electrical engineering department, at the Ecole Normale Supèrieure de l'Enseignement Technique, Mohammed V University, Rabat-Morocco

imad.aboudrar@um5s.net.ma, s.elhani@um5s.net.ma

*Imad Aboudrar, Tel: +212 671 867 920
imad.aboudrar@um5s.net.ma

Received: 01.12.2016 Accepted:11.01.2017

Abstract- This work describes a photovoltaic generator connected to the grid by associating the features of a shunt active power filter to improve the energy quality. A command by hysteresis is proposed to eliminate the harmonious currents as well as the reactive power while injecting the active power into the grid. This power is extracted by hybrid command of Maximum Power Point Tracking (MPPT) which combines the conventional Perturb and Observe (P&O) and Fractional Short Circuit Current (FSCC). The boundary condition between FSCC and P&O is intensely decided by the proposed algorithm. The use of this method allows to exploit the speed of FSCC, to put the system around the approached maximum power point (MPP), and precision of the P&O to track the real PPM with a small step of disturbance. Another advantage achieved by this method, is that it does not require any sensor to measure irradiation because it detects intelligently the change of irradiation.

Keywords FSCC, P&O, SAPF, Hybrid MPPT, PV Panel, THD, Hysteresis Command

1. Introduction

The solar energy represents an alternative energy for the electricity production because it is a renewable source, and at the same time clean, unlimited and presents a reduced level of risk [1].

Indeed, in the photovoltaic systems, the characteristic that presents a big interest is the maximal power supplied only in a single operating point called Maximal Power Point (MPP). In addition, the position of this point is not fixed, and it moves according to the irradiation and to the temperature of solar cells, therefore, the necessity of a mechanism that allows extracting the maximal power permanently. Since the 70s, a significant number of techniques of Maximum Power Point Tracking (MPPT) command were developed, by beginning with simple techniques as the MPPT controllers based on the return of state of the voltage and current [2], to more successful controllers using algorithms to calculate MPP of the PV panels,

Amongst the most used techniques [3]:

- Perturb and Observe (P&O)
- Incremental Conductance (InC)
- Fractional Short Circuit Current method (FSCC)
- Fractional Open Circuit Voltage method (FOCV)

In this paper, we propose to use a hybrid MPPT command that allows tracking the maximum power point without measuring the irradiation. [4] Have presented earlier a hybrid MPPT technique that works on the basis of P&O and FSCC for a resistive load. This technique decides intelligently about the initial operating point by using the FSCC method [5]. Therefore, it does not require any sensor to measure irradiation, so the decision about measuring the initial operation point of P&O [6] is intelligent. After finding the initial operating point, the system shifts to the conventional P&O method and starts to perturb with a small perturbation size. The use of this technique allows to the system to be fast and to work with less power oscillations [4].

However, the domestic and industrial equipment uses more and more electronics circuits with a non-linear behavior [7]. As a result they engender a non-sinusoidal harmonious current in the grid, causing harmful effects on the energy quality. In concern of optimization of the produced energy and the improvement of its quality, this work is also interested in the rejection of those harmonious by means of a Shunt Active Power Filter (SAPF) supplied by the photovoltaic generator [8].

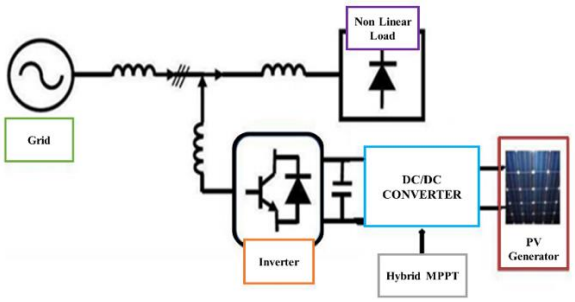

Fig. 1. Structure of the photovoltaic compensation system

2. MPPT Command

2.1. Perturb and observe P&O

The P&O method is a widely used approach in MPPT research because it is simple and requires only voltage and current measurements of the photovoltaic panel Vpv and Ipv respectively. It can detect the maximum power point even during variations of irradiation and temperature [9]. As the name suggests, the P&O method operates with Vpv voltage disturbance and observation of the impact of this change on the output power of the PV panel. If the output power has increased, Vpv is adjusted in the same direction as in the previous cycle. If the output power has decreased, Vpv is adjusted in the opposite direction. When the maximum power point is reached, Vpv oscillates around the optimal value MPP, which causes a loss of power that increases with the step of disturbance. If this step is wide, the MPPT algorithm responds quickly to sudden changes in operating conditions but engenders a loss of power [10].

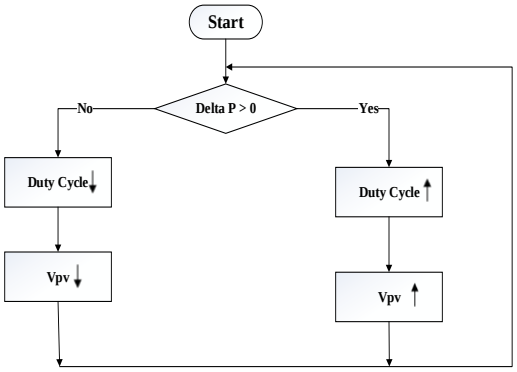

Fig. 2. Organization chart of the P&O algorithm

The problem of this method is while increasing the step of disturbance, the system becomes fast but we have an oscillation around the MPP, which causes losses of power.

2.2. Fractional short circuit current FSCC MPPT

Fractional Isc results from the fact that, under varying atmospheric conditions, Impp is approximately linearly related to the Isc of the PV array. As shown by equation1:

$$I_{mpp} = k.I_{sc} \quad (1)$$

Where k is a proportionality constant, and it vary between 0.78 and 0.92 [11]. The implementation is easy but less accurate due to the estimation of Impp. This method can be utilized for varying load applications.

The disadvantage of this method is that we do not detect the real maximal power point but just an approached point, which engenders an important oscillation around the PPM [12].

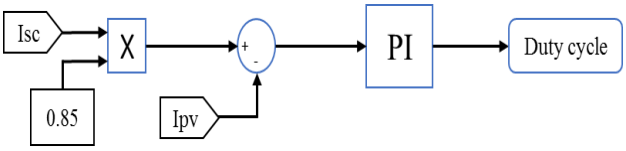

Fig. 3. Block diagram of fractional short circuit MPPT

2.3. Hybrid MPPT command

The proposed technique is designed in such a way that it revel in the advantages of both P&O and FSCC while minimizing their disadvantages. It decides intelligently about the initial operation point using the FSCC method. (This technique requires no sensor for the measure of irradiation because it detects any change of it intelligently. Consequently, the decision of measure of the initial operation point of P&O is intelligent). After having detected this approached maximum power point, the conventional method of P&O begins to perturb with a small step of disturbance until the detection of the real MPP. The use of this small step allows the system to work with fewer oscillations of power around the MPP.

The details of acronyms used in the flowchart are given below.

- k1 : Constant for estimating current at maximum power point.
- k2 : Constant of sensitivity of limit subroutine
- ΔV : Voltage step
- D : Duty cycle

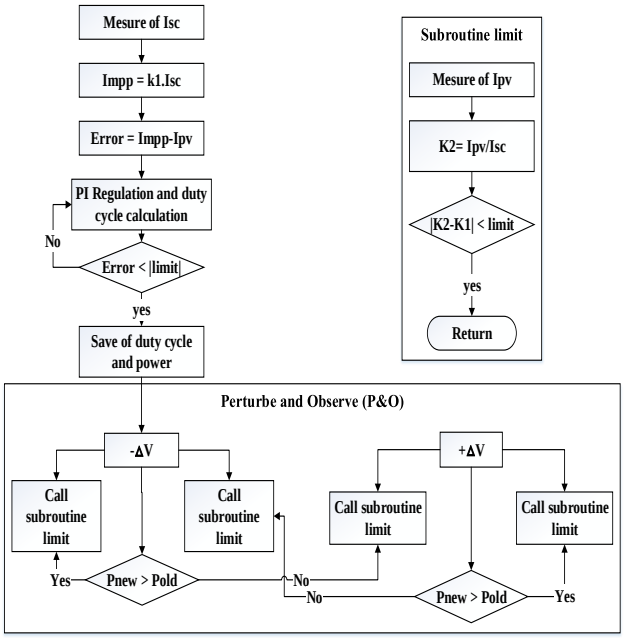

Fig. 4. Organization chart of the Hybrid MPPT algorithm[4]

3. Shunt Active Power Filter SAPF

3.1. Structure of the SAPF

The structure of a shunt active power filter decomposes into two units, power unit and control unit. The power unit consists of an inverter with switches of power, commanded in the priming and in the blocking (GTO, IGBT, etc.) with diodes in antiparallel, and of a coupling filter and a passive element that works as circuit of storage of energy, often it is a capacitor [13].

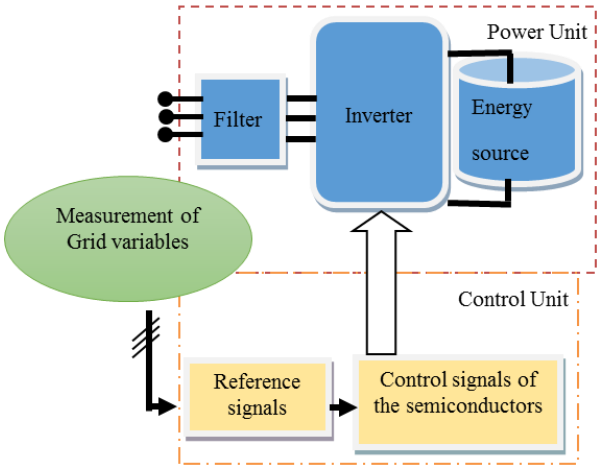

Fig. 5. General structure of a Shunt Active Power Filter

In order to compensate harmonic pollution caused by a nonlinear receiver, the SAPF consists of a DC link power converter and an energy storage element.

The control circuit performs synthesis of the reference currents of the filter in a way to compensate the undesired harmonious current components. Since the currents synthesized by the filter depends on the average voltage of the storage element, it must be kept constant. The filter control algorithm must provide this voltage control.

3.2. Control loop of the DC bus

A PI controller is used for the control of the average voltage of the storage element Vdc.

The relationship between the active power absorbed by the capacitor and the terminal voltage is:

$$P_{dc} = \frac{dW_{dc}}{dt} = \frac{d}{dt}\left(\frac{1}{2}C_{dc}V_{dc}^{2}\right) \tag{2}$$

After Laplace transformation, we have:

$$P_{dc}(p) = \frac{1}{2}pC_{dc}V_{dc}^{2}(p) \tag{3}$$

The voltage across the capacitor is given by:

$$V_{dc}^{2} = \frac{2P_{dc}(p)}{pC_{dc}} \tag{4}$$

From equation (3), and taking account of the PI controller. From a small difference between Vdc and Vdc-ref, the controller will generate the signal corresponding to the power needed to compensate losses [14] .the DC voltage control loop may then be represented by the block diagram of Fig 6:

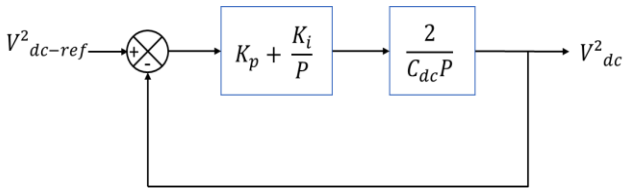

Fig. 6. Control loop for the DC voltage

The transfer function of the PI controller is:

$$C(p) = K_p + \frac{k_i}{p} \tag{5}$$

The transfer function in open loop is given by:

$$H_{OL} = (K_p + \frac{k_i}{p})\frac{2}{C_{dc}p} \tag{6}$$

The transfer function in closed loop is given by:

$$H_{CL}(p) = \frac{(1+\frac{K_p}{k_i}p)\frac{k_i}{C_{dc}}}{p^2 + \frac{K_p}{C_{dc}}p + \frac{k_i}{C_{dc}}} \tag{7}$$

By comparing equation (7) with the general shape of a transfer function of the second order given by:

$$F(p) = \frac{\omega_n{}^2}{p^2 + 2\xi\xi + \omega_n{}^2} \tag{8}$$

We have after identification:

$$k_i = \frac{1}{2}\omega_n{}^2 C_{dc}$$
$$k_p = \xi\omega_n{}^2 C_{dc} \tag{9}$$

Where

- ξ : Amortization factor
- C_{dc} : Storage Capacitor
- W_{dc} : Stored energy
- w_n : Cut-off pulsation

3.3. Estimation of the SAPF parameters:

The three main parameters to be estimated in the design of the power circuit in order to ensure adequate control and good filtering quality are [8]:

- Selection of the reference voltage value of the capacitor (V_{dcref}).
- Selection of the value of storage capacitor C_{dc}
- Selection of the filter type at the output of the inverter (L).

3.3.1. *Reference voltage* V_{dcref}

In reference [15], to ensure the current controllability of the shunt active power filter, the authors require that the DC bus voltage V_{dcref} must be above the maximum (peak) phase voltage Vs side of the inverter.

For a definite nonlinear load the following equation can be applied [16]:

$$V_{dcref} = \frac{2\sqrt{2}}{1.115} Vs \qquad (10)$$

3.3.2. *Storage capacitor* C_{dc}

For the small and average powers, the most adapted element of energy storage is a capacitor placed at the continuous side of the inverter, which has two essential spots:

- In permanent diet, it maintains the average DC link voltage constant and with low oscillations.
- It serves as an element of energy storage to compensate the difference of the real power between the load and the source during the transition periods.

The value of the capacitor C_{dc} is calculated with the following way [16]:

$$C_{dc} = \frac{I_h}{\varepsilon V_{dc} \omega_h} \qquad (11)$$

ε : Acceptable Ripple and I_h : current harmonic order h.

w_h : Pulsation of the lowest harmonic rank

3.3.3. *Output filter Lf*

In order to connect in parallel the voltage inverter with the grid, it is necessary to have a connection filter between them. The function of this filter is, firstly to convert the compensator into a current dipole from the grid point of view, and secondly to limit the dynamic of the current, to make it easier to control [8].

The value of the coupling inductor Lf is calculated as follows [16]:

$$L_f = \frac{\Delta V}{I_f \omega} \qquad (11)$$

Where ΔV represents the potential difference between the source voltage and the inverter voltage, which automatically depends on the DC bus voltage.

4. Simulation of the Photovoltaic Compensation System

The proposed compensation system acts as a reactive compensator in the case of low irradiation, and as a shunt active power filter with injection of the active power produced by the chain of photovoltaic conversion into the grid in case of a strong irradiation.

4.1. Simulation parameters

Table. 1. System Parameters

System	parameters	values
Nonlinear load (PD3 rectifier)	• Rectifier bridge with R_L load • Inductor filter	$R = 10\Omega$ $L = 1mH$ $LC = 1mH$
Grid (source of three-phase voltage)	• Efficiency Voltage • Frequency • Internal résistance • Internal inductance	$V = 50v$ $f = 50Hz$ $Rs = 0.02\Omega$ $Ls = 0.005mH$
Photovoltaic Generator Type 1STH-115	• Maximal power • Open circuit voltage • Short circuit current • Voltage at maximum power point • Current at maximum power point • Number of parallel models	$P = 115w$ $Vco = 21.8v$ $Isc = 7.5A$ $Vmpp = 17.1v$ $Impp = 6.7A$ $Np = 2$
DC/DC Chopper (Boost converter)	• Input Capacitor • Input inductor • IGBT semiconductor	$Cin = 20\mu F$ $l = 1.5mH$
Shunt active power filter	• Capacitor of DC bus • Output Filter • reference Voltage • Hysteresis Band • PI Controller parameters	$Cdc = 1300\mu F$ $Lf = 1mH$ $Vdref = 120v$ $HB = 0.1A$ $Ki = 22$ $Kp = 0.2$

4.2. Simulation results

4.2.1. *Simulation before introduction of the photovoltaic compensation system*

- Load Current Ic

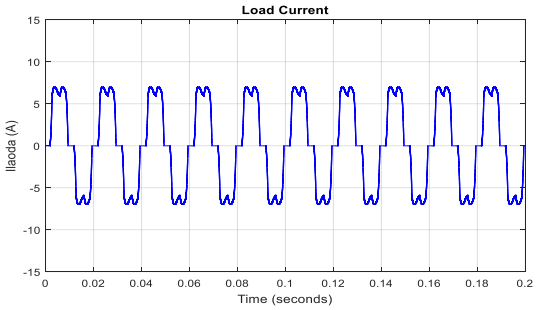

Fig. 8. Waveforms of the current load

- Source current Is

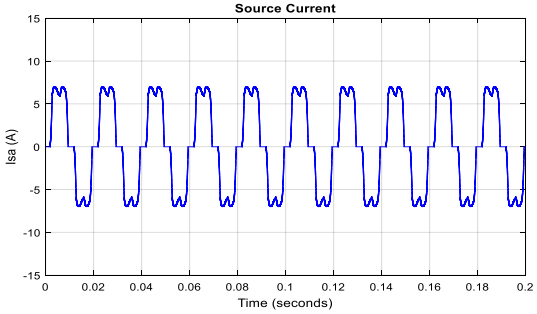

Fig. 9. Waveforms of the currents Is before photovoltaic compensation

- Active power consumed

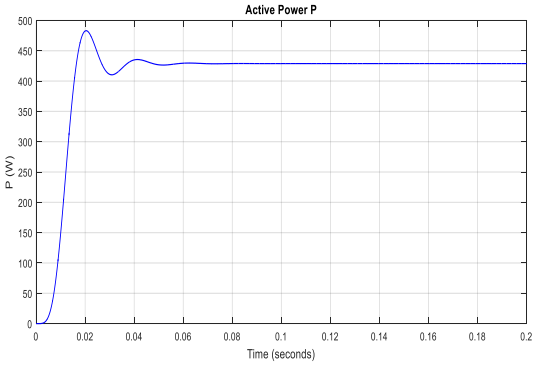

Fig. 10. Active power consumed before compensation

- Reactive power consumed

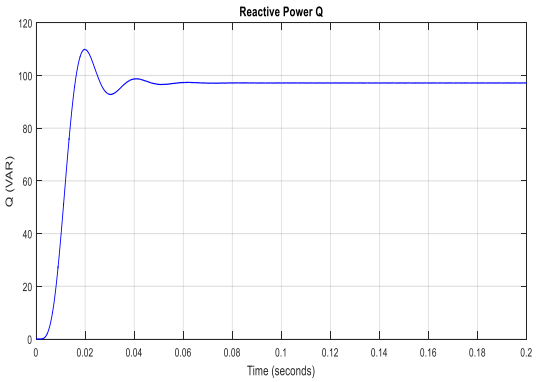

Fig. 11. Reactive power consumed before photovoltaic compensation

- Harmonious distortion THD

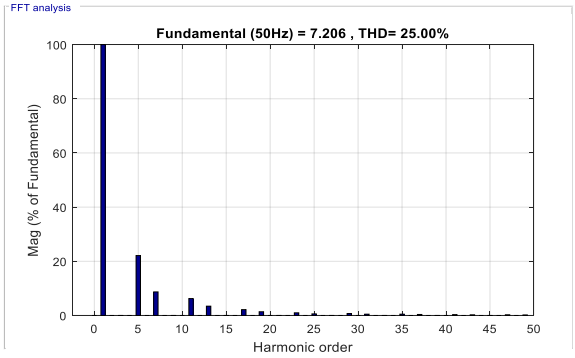

Fig. 12. Spectral analysis of the source current before the introduction of the photovoltaic compensation system

Initially the system works without the photovoltaic compensation system. The load consumes active power of 430W and the source currents **Is** are identical to those of the nonlinear load **Ic,** wich are characterized by a spectrum containing only odd order harmonics (not multiple of three) and with a rate of harmonious distortion of THD = 25%.

4.2.2. Simulation after introduction of the photovoltaic compensation system

- Source current Is

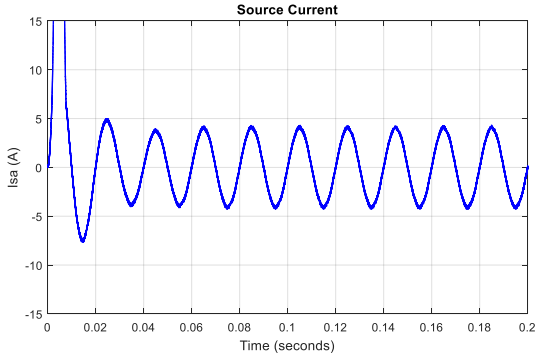

Fig. 13. Waveforms of the currents Is after photovoltaic compensation

- Current injected by the filter If

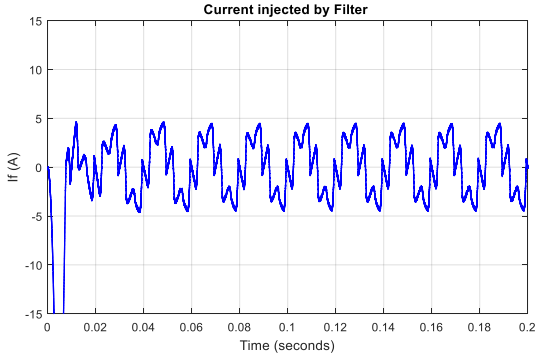

Fig. 14. Waveforms of the compensation currents injected in the grid

- Power supplied by the photovoltaic panel

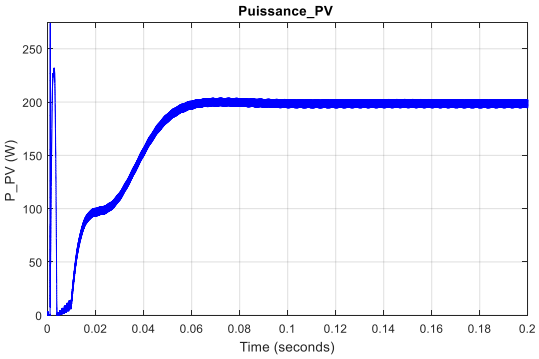

Fig. 15. Power provided by the photovoltaic panel by hybrid MPPT

- Vdc and Vdcréf voltage

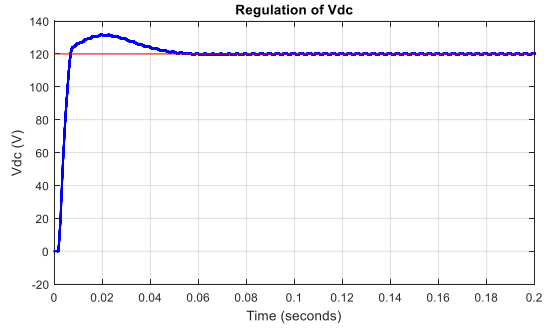

Fig. 16. Regulation of the Vdc with the PI controller

- Active power consumed

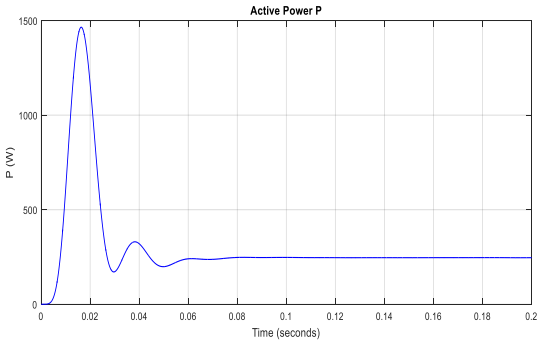

Fig. 17. Active power consumed after the implementation of the PV compensation system

- Reactive power consumed

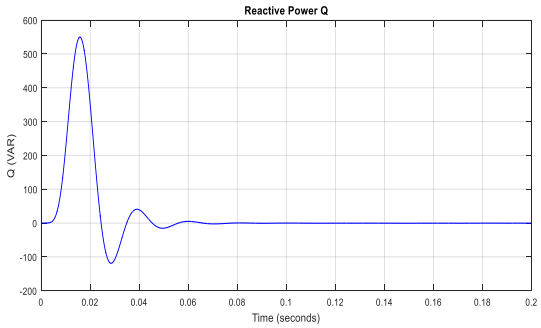

Fig.18. Reactive power consumed after the implementation of the PV compensation system

- Harmonious distortion THD

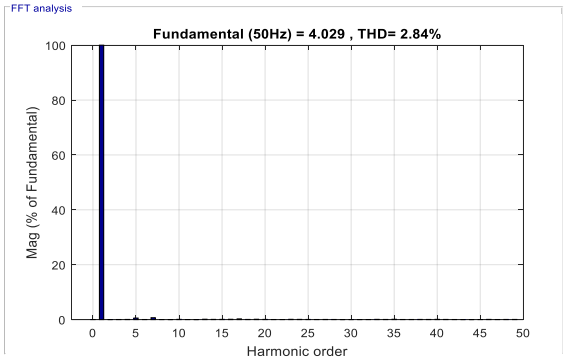

Fig. 19. Spectral analysis of the source current after the introduction of the photovoltaic compensation system

- Vs and current Is

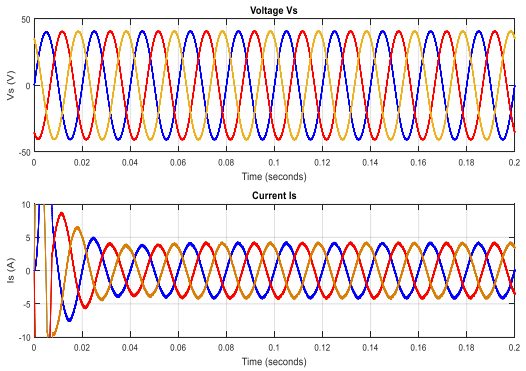

Fig. 20. Voltage (vs) and current (is) after filtering

Those figures shows that the SAPF was put into service, by producing a current **If** that arrives after passing on transitional phase of 0.06s, and it makes the source currents sinusoidal and in phase with the corresponding voltages. After the transitional, we also see that the active power decreases which is due to the injection of the photovoltaic power produced by the panels into the grid, while the reactive energy is around zero. So, the rate of harmonious distortion of the current source is improved and it is equal to THD=2.84 %.

5. Conclusion

This work presents the study of a harmonic compensation system using Of a PV system. The main objective of this system, which is composed of a SAPF and a GPV, is to compensate the disturbances generated by the non-linear loads such as the harmonic currents, reactive power and inject the active powers Produced by the PV conversion chain. The extraction of the maximum PV power was done by a hybrid MPPT, which based on two MPPT methods P&O and FSCC. In concern to control the DC bus voltage, the choice was made for a conventional PI controller, which proved its performance in terms of stability and robustness for this application. The simulation results obtained confirm the theoretical study, and in particular the efficiency and the robustness of the proposed system: a quasi-sinusoidal current with a rate of harmonious distortion THD=2.84.

However, the work presented in this paper opens wide perspectives in the field of active filtering associated with renewable energies. We can mentions:

- For the identification of different perturbations by using the instantaneous active and reactive powers theory instead of the frequency theory which requires a high computation time. Other advanced algorithms such as neural, neuro-fuzzy networks can also be envisaged.
- For real-time control: we can use the FPGA for the hardware implementation in concern of comparing the results.
- For the MPPT command, we can consider using advanced methods such as those based on neural networks and genetic algorithms.

References

[1] LIANG, Zhigang, GUO, Rong, LI, Jun, et al. A high-efficiency PV module-integrated DC/DC converter for PV energy harvest in FREEDM systems. IEEE Transactions on Power Electronics, 2011, vol. 26, no 3, p. 897-909.

[2] SALAS, V., OLIAS, E., BARRADO, A., et al. Review of the maximum power point tracking algorithms for stand-alone photovoltaic systems. Solar energy materials and solar cells, 2006, vol. 90, no 11, p. 1555-1578.

[3] ESRAM, Trishan, CHAPMAN, Patrick L., et al. Comparison of photovoltaic array maximum power point tracking techniques. IEEE Transactions on Energy Conversion EC, 2007, vol. 22, no 2, p. 439.

[4] SHER, Hadeed Ahmed, MURTAZA, Ali Faisal, NOMAN, Abdullah, et al. A New sensorless hybrid MPPT algorithm based on fractional short-circuit current measurement and P&O MPPT. IEEE Transactions on Sustainable Energy, 2015, vol. 6, no 4, p. 1426-1434.

[5] BERRERA, M., DOLARA, A., FARANDA, R., et al. Experimental test of seven widely-adopted MPPT algorithms. In : PowerTech, 2009 IEEE Bucharest. IEEE, 2009. p. 1-8.

[6] JIANG, Joe-Air, HUANG, Tsong-Liang, HSIAO, Ying-Tung, et al. Maximum Power Tracking for Photovoltaic Power Systems. Tamkang Journal of Science and Engineering, 2005, vol. 8, no 2, p. 147r153.

[7] AL CHAER, Toufic, GAUBERT, Jean-Paul, RAMBAULT, Laurent, et al. Linear feedback control of a parallel active harmonic conditioner in power systems. IEEE Transactions on Power Electronics, 2009, vol. 24, no 3, p. 641-653.

[8] CHAOUI, Abdelmadjid, GAUBERT, Jean-Paul, KRIM, Fateh, et al. IP controlled three-phase shunt active power filter for power improvement quality. In : IECON 2006-32nd Annual Conference on IEEE Industrial Electronics. IEEE, 2006. p. 2384-2389.

[9] KOLLIMALLA, Sathish Kumar et MISHRA, Mahesh Kumar. A new adaptive P&O MPPT algorithm based on FSCC method for photovoltaic system. In : Circuits, Power and Computing Technologies (ICCPCT), 2013 International Conference on. IEEE, 2013. p. 406-411.

[10] FEMIA, Nicola, PETRONE, Giovanni, SPAGNUOLO, Giovanni, et al. Optimization of perturb and observe maximum power point tracking method. IEEE transactions on power electronics, 2005, vol. 20, no 4, p. 963-973.

[11] REISI, Ali Reza, MORADI, Mohammad Hassan, et JAMASB, Shahriar. Classification and comparison of maximum power point tracking techniques for photovoltaic system: A review. Renewable and Sustainable Energy Reviews, 2013, vol. 19, p. 433-443.

[12] SHER, Hadeed A., MURTAZA, Ali F., ADDOWEESH, Khaled E., et al. A new irradiance sensorless hybrid MPPT technique for photovoltaic power plants. In : IECON 2014-40th Annual Conference of the IEEE Industrial Electronics Society. IEEE, 2014. p. 1919-1923.

[13] DEWEZ, Claude. Modélisation d'un filtre actif parallèle triphasé pour la dépollution harmonique et synthèse d'une commande basée sur le rejet de perturbations. 2007. Thèse de doctorat. Université de Poitiers. UFR des sciences fondamentales et appliquées.

[14] ZHENG, Zeng, JIAQIANG, Yang, et NIANCHANG, Yu. Research on PI and repetitive control strategy for Shunt Active Power Filter with LCL-filter. In : Power Electronics and Motion Control Conference (IPEMC), 2012 7th International. IEEE, 2012. p. 2833-2837.

[15] DAI, Ning-Yi et WONG, Man-Chung. Design considerations of coupling inductance for active power filters. In : 2011 6th IEEE Conference on Industrial Electronics and Applications. IEEE, 2011. p. 1370-1375.

[16] CHAOUI, Abdelmadjid. Filtrage actif triphasé pour charges non linéaires. 2010. Thèse de doctorat. École nationale supérieure d'ingénieurs (Poitiers).